Electronic Supplementary Material (ESI) for ChemComm.

Supporting Information

Broadband red emission from one-dimensional hexamethonium lead bromide perovskitoid

Biqi He,[a] Kuan Kuang,[a] Bing Xu[b], Junjie Tang,[a] Sheng Cao,[a] Zixian Yu,[a] Mingkai Li*[a], Yunbin He*[a], Junnian Chen*[a]

[a.]Ministry-of-Education Key Laboratory of Green Preparation and Application for Functional Materials, and School of Materials Science & Engineering, Hubei University, Wuhan 430062, China
[b.]Lingnan Normal University, Zhanjiang, 524048, China
*Corresponding authors.

Experimental section

Materials. Hexamethonium bromide, $Pb(Ac)_2 \cdot 3H_2O$ (99.998%), hydrobromic acid (48 wt.% in H_2O) were purchased from Aladdin Industrial Inc. All reagents were purchased from Aladdin and used as received.

Synthesis of 1D (HM)Pb_2Br_6 bulk crystals. $Pb(Ac)_2 \cdot 3H_2O$ (1 mmol, 0.3793g) and hexamethonium bromide (1 mmol, 0.3622 g) were dissolved in 6.5 mL of 48 wt.% hydrobromic acid under heating at 120 ℃ in a methyl silicone oil bath with stirring until a clear solution formed. After that, the precursor solution was cooled to room temperature at a rate of 5°C/h, yielding colorless prismatic crystals.

Characterization. The Single-crystal X-ray diffraction data were performed on a Bruker D8 Venture diffractometer with rotating anode (Mo-Kα radiation). The structure data was solved and refined using SHELXT and Olex2. Powder X-ray diffraction (PXRD) patterns were collected using a Bruker D8 Advance powder X-ray diffractometer (D8 ADVANCE, Bruker) with Cu Kα radiation. Optical absorption spectra were recorded using a UV−Vis−NIR pectrophotometer (UV-3600 Plus, Shimadzu). Raman spectra were acquired with 532 nm laser, using a Horiba LabRAM HR Evolution. The morphology and elemental mapping images of (HM)Pb_2Br_6 were measured by the SIGMA 500 field emission scanning electron microscope (FE-SEM, Zeiss, Germany). Steady-state PL spectra, temperature-dependent photoluminescence spectra of the perovskites, time-resolved photoluminescence (TRPL) and photoluminescence quantum yields (PLQYs) were measured using an FLS980 spectrofluorometer (Edinburgh Instruments Ltd.). The light intensity-dependent photoluminescence measurement was carried out using a spectrofluorometer (Fluo Time 300) with 375 nm laser.

Calculated methods. Density functional theory (DFT) calculations were conducted with the Vienna ab initio Simulation Package (VASP) to study the electronic structure. The Perdew-Burke-Ernzerhof (PBE) generalized gradient approximation (GGA) functional correlated with spin-orbit coupling (SOC) corrections was considered for all the calculations. Additionally, the energy cutoff was set at 500 eV and a 4 × 5 × 2 k-

point mesh was built in the first Brillouin zone integration. The value of energy and force convergence were 10^{-7} eV and 0.01 eV/Å. To survey the origin of self-trapped charges, four possible structures were designed by decreasing the corresponding bond lengths. Partial charge densities of VBM and CBM were calculated to describe their hole and electron densities distribution in these four situations. The crystal structure and charge densities graphs were plotted by the software visualization for electronic and structural analysis (VESTA).

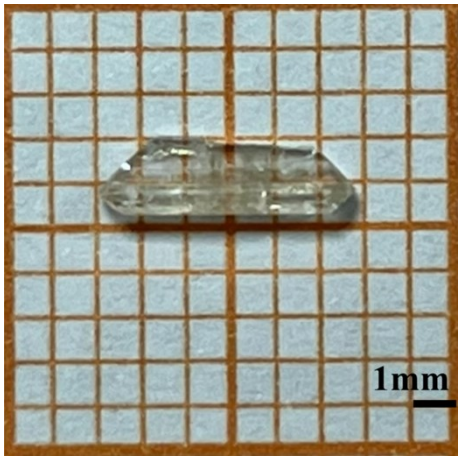

Figure S1. Photograph of the bulk single crystal of (HM)Pb_2Br_6. It shows prism morphology with a size of 6×2×1 mm^3.

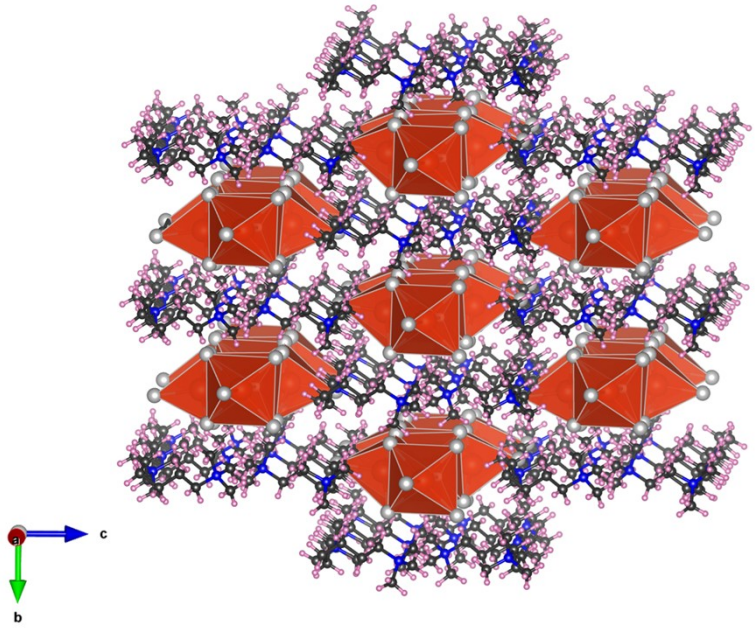

Figure S2. The side view of (HM)Pb_2Br_6 crystal structure along the a-axis.

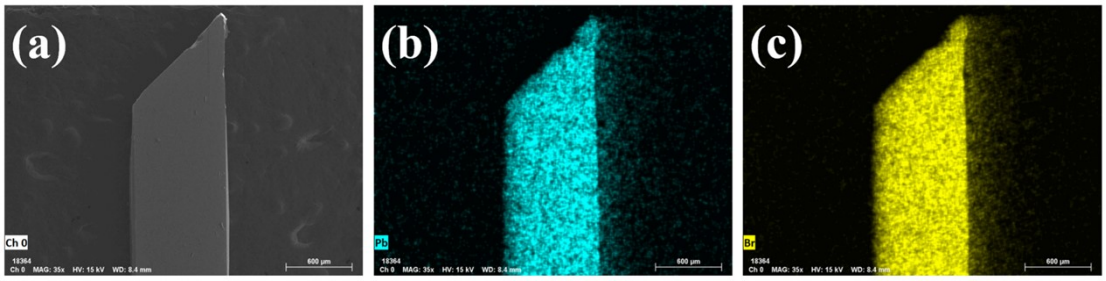

Figure S3. (a) The SEM image of (HM)Pb_2Br single crystal. The EDS elemental mapping images of (b) Pb and (c) Br elements of (HM)Pb_2Br_6 single crystal.

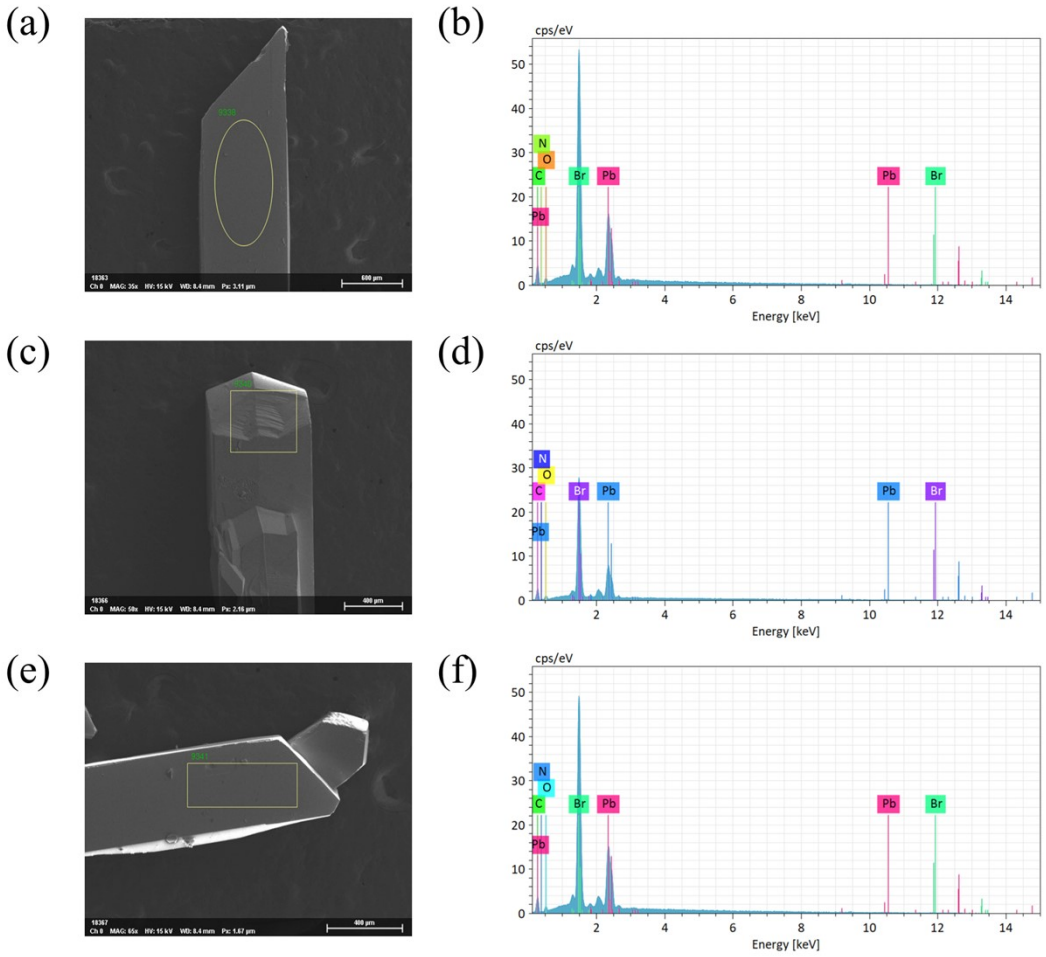

(g)

	Point 1		Point 2		Point 3		Average	
	Pb	Br	Pb	Br	Pb	Br	Pb	Br
Atom%	8.16	27.79	6.67	25.60	8.43	29.31	/	/
Ratio	1	3.41	1	3.84	1	3.48	1	3.58

Figure S4. The SEM images of (HM)Pb_2Br_6 (a, c and e) and the corresponding EDS spectrum (b, d and f). (g) The contents of Pb and Br elements obtained from EDS spectra.

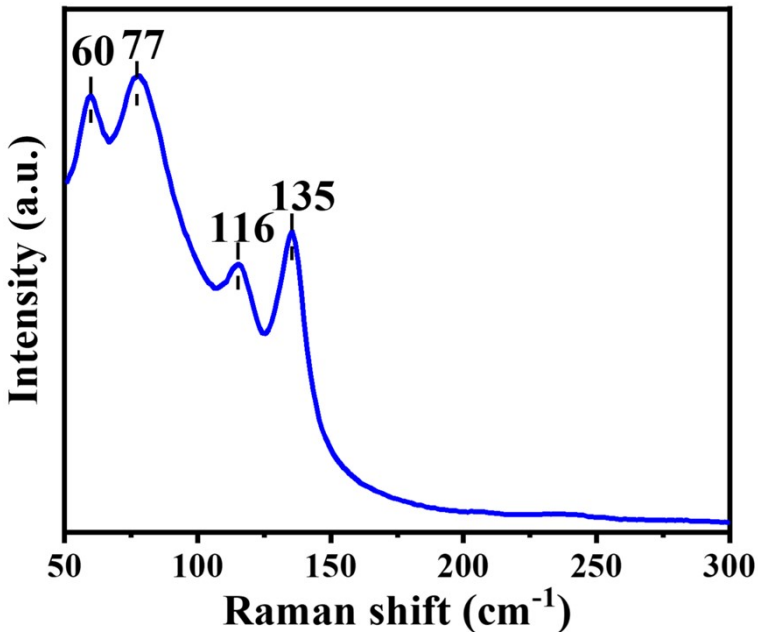

Figure S5. Raman spectra of $(HM)Pb_2Br_6$ in the range 50-300 cm^{-1} under excitation of 532 nm laser. The Raman peaks located at 60 and 77 cm^{-1} are assigned as the bending modes of the Br−Pb-Br framework, and the sharp peaks located at 116 and 135 cm^{-1} are ascribed to the symmetric stretching vibrations of the Pb−Br bond respectively.

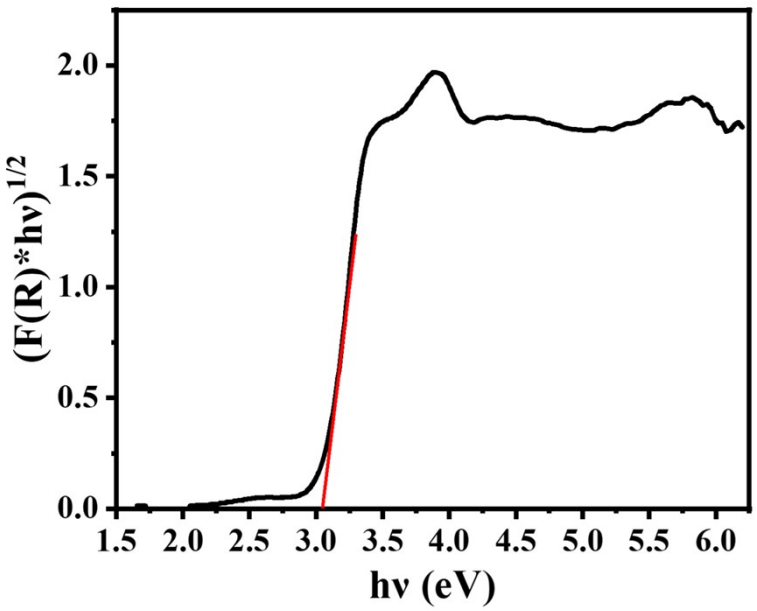

Figure S6. Plot of $(F(R)*h\nu)^{1/2}$ versus hν for $(HM)Pb_2Br_6$. The optical bandgap of $(HM)Pb_2Br_6$ is estimated as 3.05 eV as an indirect bandgap using the function of $(F(R)*h\nu)^{1/2}$.

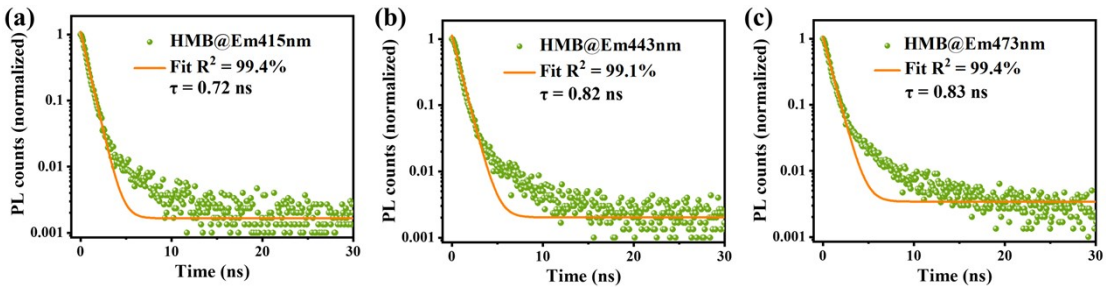

Figure S7. Time-resolved PL decay curves of $HMBr_2$ collected at (a) 415 nm, (b) 443 nm and (c) 473 nm emission wavelength at room temperature.

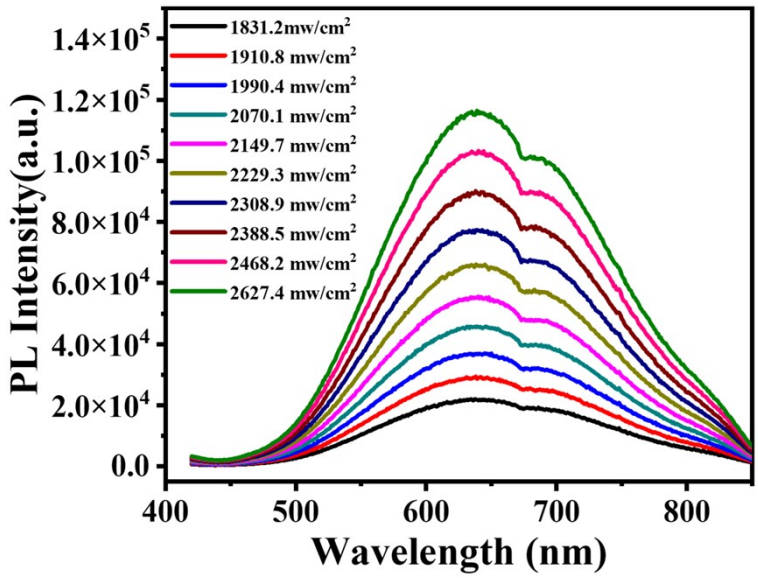

Figure S8. PL spectrum of $(HM)Pb_2Br_6$ as a function of excitation power. The PL intensity exhibits significant decrease as the optical power increases.

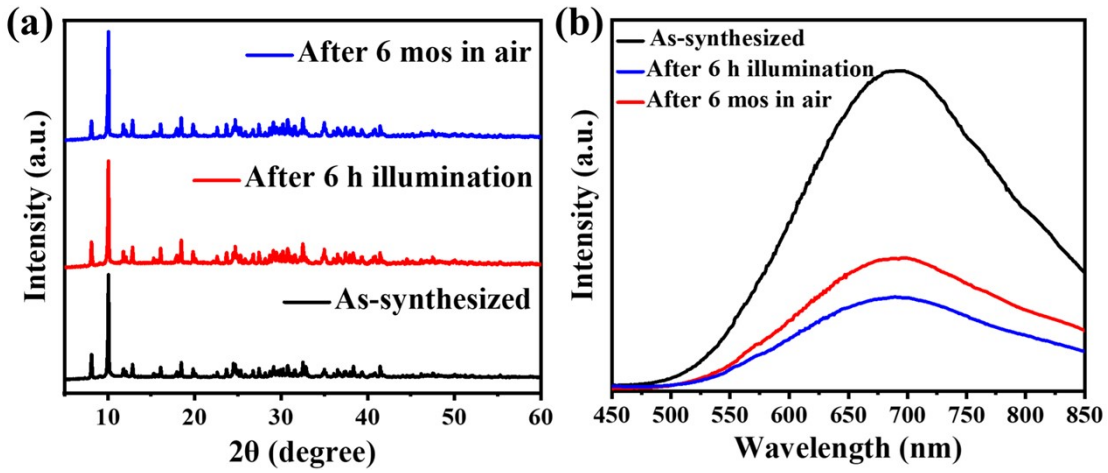

Figure S9. (a) XRD patterns and (b) PL stability of the as-synthesized, after storage for 6 months in air or after illumination under high-power UV lamp (300 W) for 6 h, indicating high structure stability.

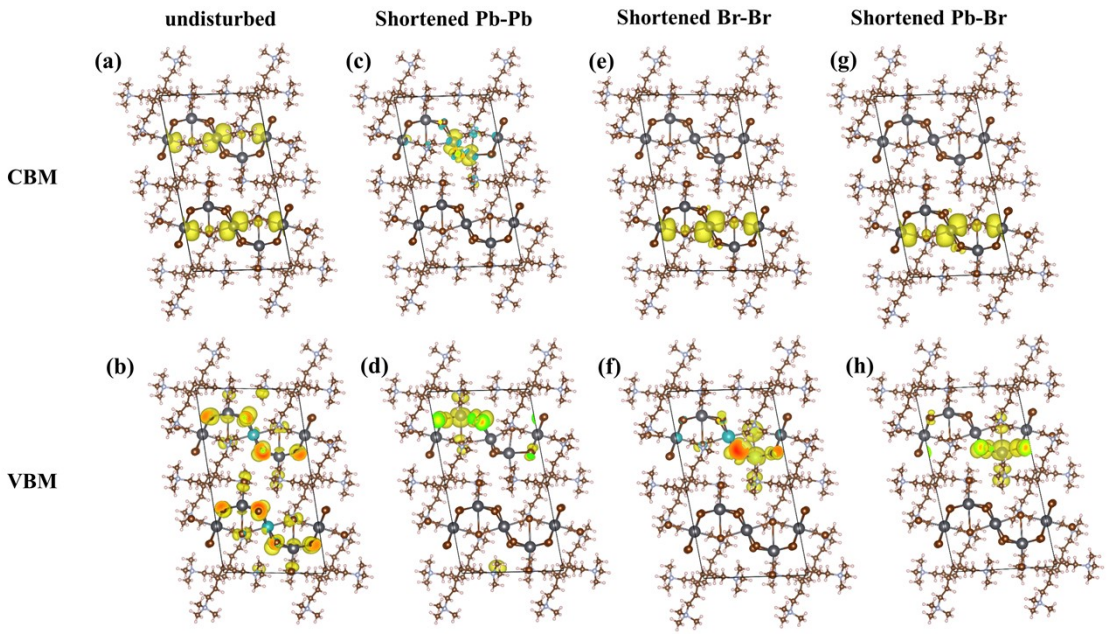

Figure S10. Plots of charge-density distributions of (HM)Pb_2Br_6 for VBM and CBM calculated at the PBE/wSOC level. The CBM and VBM structures of (HM)Pb_2Br_6 is undisturbed (a, b) and disturbed undergoing shortening of the following atomic distances: Pb−Pb (c, d), Br-Br (e, f), Pb-Br (g, h). In the unperturbed structure, the charges are fully delocalized in the inorganic lead bromide framework compared to strong charge localization upon disturbation.

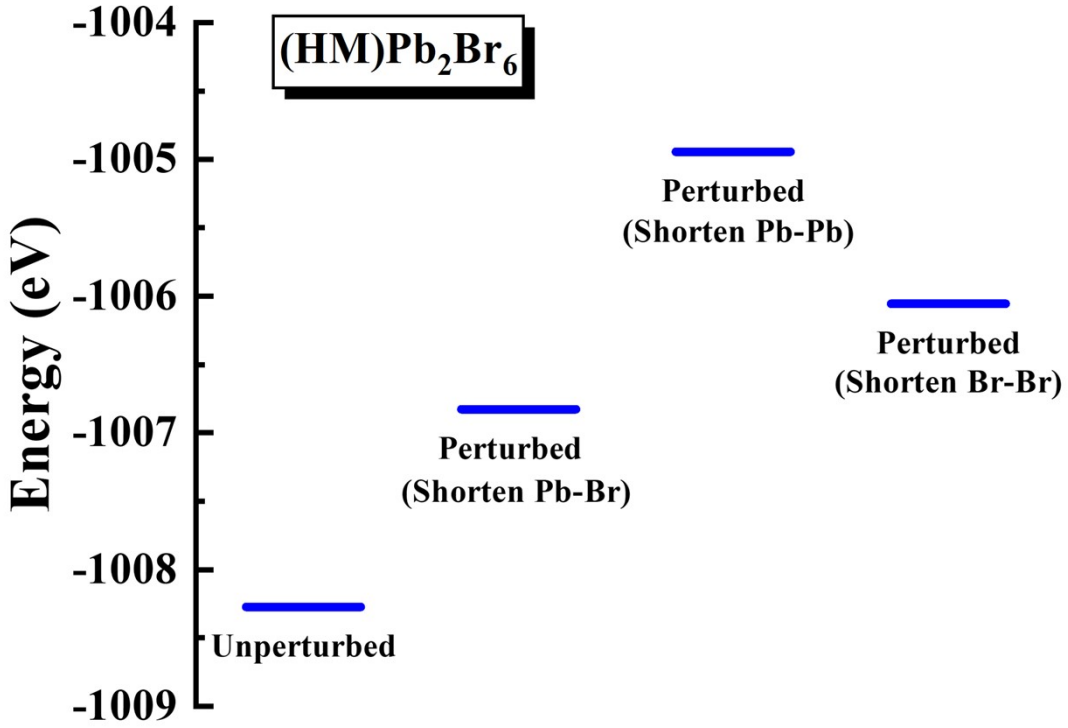

Figure S11. Energy for the unperturbed and perturbed structure of (HM)Pb_2Br_6 calculated at the PBE/wSOC level.

Table S1. Crystal data and structure refinement of $(HM)Pb_2Br_6$ at 298K.

Compound	**$(HM)Pb_2Br_6$**
Empirical formula	$C_{12}H_{30}Br_6N_2Pb_2$
Formula weight	1096.22
Temperature/K	298.00
Crystal system	monoclinic
Space group	P2/c
a/Å	12.1162(2)
b/Å	9.5440(2)
c/Å	22.0199(5)
α/°	90
β/°	99.2890(10)
γ/°	90
Volume/Å^3	2512.92(9)
Z	4
ρ_{calc}g/cm^3	2.898
μ/mm^{-1}	22.921
F(000)	1960.0
2θ range for data collection/°	3.406 to 54.944
Index ranges	$-15 \leq h \leq 14$, $-7 \leq k \leq 12$, $-28 \leq l \leq 28$
Reflections collected	25084
Independent reflections	5720 [R_{int} = 0.1058, R_{sigma} = 0.0945]
Data/restraints/parameters	5720/171/206
Goodness-of-fit on F^2	1.061
Final R indexes [I>=2σ (I)]	R_1 = 0.0577, wR_2 = 0.1285
Final R indexes [all data]	R_1= 0.0927, wR_2 = 0.1508
Largest diff. peak/hole / e Å^{-3}	2.97/-4.60

Table S2. Selected Pb-Br bond lengths [Å] for (HM)Pb_2Br_6.

Atom-Atom	Length / Å	Atom-Atom	Length / Å
Pb1-Br1[1]	2.9499(11)	Pb2-Br5	2.8138(14)
Pb1-Br1	2.9499(11)	Pb2-Br6	2.9799(12)
Pb1-Br2[1]	3.1611(16)	Pb3-Br2	3.1416(15)
Pb1-Br2	3.1611(16)	Pb3-Br2[2]	3.1416(15)
Pb1-Br4	3.0644(11)	Pb3-Br3[2]	3.0231(12)
Pb1-Br4[1]	3.0644(11)	Pb3-Br3	3.0231(12)
Pb2-Br1	3.1316(12)	Pb3-Br6[2]	3.0192(11)
Pb2-Br3	3.1441(12)	Pb3-Br6	3.0192(11)
Pb2-Br4	2.9569(11)		

[1]1-X,+Y,3/2-Z; [2]2-X,+Y,3/2-Z

Table S3. Selected Br-Pb-Br bond angles [°] for (HM)Pb_2Br_6.

Atom–Atom–Atom	Angle / °	Atom–Atom–Atom	Angle / °
$Br1^1$-Pb1-Br1	99.33(4)	Br5-Pb2-Br3	106.48(4)
$Br1^1$-Pb1-$Br2^1$	86.81(4)	Br5-Pb2-Br4	93.87(4)
Br1-Pb1-$Br2^1$	89.59(4)	Br5-Pb2-Br6	97.34(4)
$Br1^1$-Pb1-Br2	89.59(4)	Br6-Pb2-Br1	163.83(4)
Br1-Pb1-Br2	86.81(4)	Br6-Pb2-Br3	84.82(3)
$Br1^1$-Pb1-$Br4^1$	86.96(3)	Br2-Pb3-$Br2^2$	178.60(5)
Br1-Pb1-Br4	86.96(3)	$Br3^2$-Pb3-$Br2^2$	85.19(3)
$Br1^1$-Pb1-Br4	169.29(4)	$Br3^2$-Pb3-Br2	95.73(3)
Br1-Pb1-$Br4^1$	169.28(4)	Br3-Pb3-$Br2^2$	95.73(3)
$Br2^1$-Pb1-Br2	174.44(4)	Br3-Pb3-Br2	85.20(4)
Br4-Pb1-$Br2^1$	101.99(3)	$Br3^2$-Pb3-Br3	97.60(5)
$Br4^1$-Pb1-Br2	101.99(3)	Br6-Pb3-Br2	86.97(3)
Br4-Pb1-Br2	82.06(3)	$Br6^2$-Pb3-Br2	92.04(3)
$Br4^1$-Pb1-$Br2^1$	82.06(3)	Br6-Pb3-$Br2^2$	92.04(3)
$Br4^1$-Pb1-Br4	88.22(4)	$Br6^2$-Pb3-$Br2^2$	86.97(3)
Br1-Pb2-Br3	91.56(3)	$Br6^2$-Pb3-Br3	175.42(3)
Br4-Pb2-Br1	85.61(3)	$Br6^2$-Pb3-$Br3^2$	86.30(3)
Br4-Pb2-Br3	159.64(4)	Br6-Pb3-Br3	86.29(3)
Br4-Pb2-Br6	92.31(3)	Br6-Pb3-$Br3^2$	175.42(3)

Br5-Pb2-Br1	98.81(4)	Br6-Pb3-Br6^2	89.92(4)

Table S4. Summary of distortion Index (Δd) of "PbX_6" octahedra and bond angle variance (σ^2).

Compound	$\Delta d_{Pb}1$ ($\times 10^{-5}$)	$\Delta d_{Pb}2$ ($\times 10^{-5}$)	$\Delta d_{Pb}3$ ($\times 10^{-5}$)	Δd_{avg} ($\times 10^{-5}$)	$\sigma^2_{Pb}1$	$\sigma^2_{Pb}2$	$\sigma^2_{Pb}3$	σ^2_{avg}
$(HMB)Pb_2Br_6$	79.7	334	34.4	149	49	74	20	48